TEMPERATURES AND THERMOPHYSICAL PROPERTIES OF THE LUNAR OUTERMOST LAYER

WILLIAM P. JONES, JAMES R. WATKINS, and TED A. CALVERT
Space Sciences Laboratory, NASA Marshall Space Flight Center, Huntsville, Ala., U.S.A.

(Received 12 May, 1975)

Abstract. Comparisons of calculated diurnal and eclipse temperatures of the lunar outermost layer are made with Earth-based infrared and millimeter data. The thermophysical model upon which the calculations are based incorporates variable physical properties. The thermal conductivity is a function of both density (depth) and temperature; the specific heat is a function of temperature; the density is a function of depth; and the dielectric constant and loss tangent are functions of density (depth). Laboratory measurements and Apollo sample results are incorporated in the property data. Calculational cases are based largely upon different density profiles. The model is consistent with the data, and the comparisons of theoretical and observational temperatures are very favorable. For such comparisons, further sophistication of the thermophysical model of the outermost layer is probably not justified.

1. Introduction

The problem of constructing a theoretical model which may be used to calculate lunar temperatures as a function of depth and time and which compares satisfactorily with observational temperatures determined from infrared lunation, infrared eclipse, and microwave lunation measurements has been one of considerable interest, beginning, perhaps, with Epstein's (1929) effort to compare calculated temperatures with those determined from Pettit's and Nicholson's (1930) eclipse observations. After early efforts, there arose the difficulty of constructing a single model which would explain both the infrared lunation and eclipse data as well as the millimeter data, as opposed to models which would explain only one or two of these three categories of measurements. The various attempts to construct adequate theoretical models ranging from Wesselink's (1948) famous paper to the more recent ones of Linsky (1966) and Winter and Saari (1969) are surveyed in several papers (Weaver, 1965; Troitskiy, 1965; Jones, 1969; Troitskiy *et al.*, 1971) and will not be reviewed further here.

The purposes of this paper are to: (1) present the results from a model proposed earlier in outline form by one of the authors (Jones, 1969) in which the thermal conductivity is a function of both depth and temperature, the density is a function of depth, the specific heat is a function of temperature, and the dielectric 'constant' and loss tangent are functions of depth, with all of these being continuous functions; (2) give briefly the computational and numerical methods used; (3) show that the calculated results yielded by the model compare well with both the infrared and millimeter observational data; and (4) illustrate that the results are not inconsistent with the recent data on physical properties from the Apollo program.

The observational data used for comparison with the theoretical results of this work are those of Murray's and Wildey's (1963, 1964) nighttime infrared, Mendell's and

The Moon **13** (1975) 475–494.

Low's recent (1970) nighttime infrared, Shorthill's and Saari's (1965, 1967) eclipse infrared, Winter's (1968) summary of infrared, and Ulich *et al.*'s (1974) recent millimeter lunation.

Prior to the model presented here, the Winter and Saari (1969) model came closer to satisfying the known requirements. But, that model had the following deficiencies: (1) the density was constant, (2) the conductive component of the thermal conductivity was a function of depth only, while the radiative component was a function of temperature only, (3) the absorption coefficient, dielectric constant, and loss tangent were constant, and (4) the comparison with the millimeter observational data was not completely satisfying. Moreover, additional infrared lunation data further into the lunar night (Mendell and Low, 1970), additional millimeter data (Ulich *et al.*, 1974), and data on physical properties from the Apollo program have become available. The present model satisfies these additional requirements as well as the long-standing ones.

2. The Theoretical Model

The fundamental description of the model for calculating the temperatures of the Moon as a function of depth and time is stated as a boundary value-initial condition problem in partial differential equations in the form for a semi-infinite solid. The model consists of the one space dimensional, nonlinear, nonhomogeneous, parabolic partial differential equation of heat conduction; the usual boundary condition at depth for the semi-infinite solid; initial conditions in time; a distinction in time between the lunation and eclipse cases; and auxiliary equations for the thermophysical properties.

The appropriate partial differential equation (*pde*) is

$$\varrho(x)\, c(T) \frac{\partial T}{\partial t} = \frac{\partial}{\partial x}\left[k(x, T) \frac{\partial T}{\partial x}\right], \tag{1}$$

where $\varrho(x)$ is bulk density as a function of depth, x; $c(T)$ is specific heat as a function of temperature, T; and $k(x, T)$ is thermal conductivity as a function of depth and temperature. (The units of physical quantities in this paper are the *Système International d'Unités*, designated SI in all languages.)

The surface boundary condition is

$$F(t) - \varepsilon\sigma T^4 = -\lim_{x \to 0}\left[k(x, T) \frac{\partial T}{\partial x}\right], \tag{2a}$$

where ε is the radiative emittance of the lunar surface, σ is the Stefan-Boltzmann physical constant, and

$$F(t) = E(t/P)\, \alpha S r^2 \cos(2\pi t/P) \cos\phi\,. \tag{2b}$$

In this definition of $F(t)$, α is the absorptance of the lunar surface with respect to solar incident radiation; r is the reciprocal of the ratio of the distance from the Earth to the Sun at a particular time to the nominal value of this distance; t is the time in a

lunation measured from zero time taken arbitrarily as local noon; P is the time of a lunation period (nominally equal to 708.73416 hours); ϕ is selenographic latitude; S is the solar constant; and

$$S = \begin{cases} 1353 \text{ W m}^{-2}, \text{ if } 0 \leqslant t \leqslant P/4 \\ 0, \quad \text{if } P/4 < t < 3P/4 \\ 1353 \text{ W m}^{-2}, \text{ if } 3P/4 \leqslant t \leqslant P. \end{cases} \tag{2c}$$

$E(t/P)$ is an eclipse function ($0 \leqslant E(t/P) \leqslant 1$) which modifies the solar incidence for a particular eclipse and lunar location and which is represented for calculational purposes by cubic splines.

The lower boundary condition is

$$\lim_{x \to \infty} T(x, t) = V, \text{ a constant}. \tag{3}$$

Initial conditions are obtained from a Fourier series solution to the linear, homogeneous problem (Calvert, 1969) and are given by

$$T(x, 0) = \left\{ A_0 + \sum_{n=1}^{50} e^{-x\sqrt{n\pi/\alpha^* P}} \left[A_n \cos\left(-x\sqrt{n\pi/\alpha^* P}\right) + \right. \right. \\ \left. \left. + B_n \sin\left(-x\sqrt{n\pi/\alpha^* P}\right) \right] \right\} \cos^{1/4}\phi, \tag{4}$$

where A_0, A_n, and B_n are the Fourier coefficients determined from infrared lunation observations and α^* is the thermal diffusivity (defined only for constant thermal conductivity – here, only for estimating the initial conditions) of the lunar surface, taken to be constant and equal to 0.4576×10^{-4} m^2 h^{-1} for purposes of calculating the initial temperature profile.

The bulk density profile is assumed to be represented by a density-depth model proposed earlier (Jones, 1968) having the form

$$\varrho(x) = \varrho_\infty \Big/ \left[1 + \left(\frac{\varrho_\infty}{\varrho_0} - 1 \right) e^{-x/x^*} \right], \tag{5a}$$

where $\varrho_0 = \lim_{x \to 0} \varrho(x)$; $\varrho_\infty = \lim_{x \to \infty} \varrho(x)$; and x^* is a parameter determined by

$$x^* = -x_{\text{int}} / \ln\left[\varrho_0(\varrho_\infty - \varrho_{\text{int}}) / \varrho_{\text{int}}(\varrho_\infty - \varrho_0)\right], \tag{5b}$$

in which the interior point $(x_{\text{int}}, \varrho_{\text{int}})$ is assumed in order to obtain a particular profile. Since the actual density-depth profile of the Moon is unknown, this profile becomes the primary free choice to distinguish between computational cases. As will be seen, all other physical properties and parameters in the theoretical temperature model presented here are essentially fixed by other considerations.

Buettner (1963), in an early paper, proposed that the thermal conductivity of particulate material (basalt, in that case) in vacuum be represented by $k = \text{constant} + \text{constant} \cdot T^3$. Later analysis based upon heat transfer in vacuum (Watson, 1964), laboratory measurements (Wechsler, 1966), radiative transfer in stellar atmospheres

(Wildey, 1967), and porosity of particulate materials (Halajian, 1967) supported Buettner's proposal. Since this form for the conductivity was based upon a physically homogeneous material in both the theoretical and laboratory verifications of the form, and, considering the necessity for the function, $\varrho(x)$, it became evident (Jones, 1969) that the conductivity could, and probably should, be represented by

$$k(x, T) = k_0(x) + k_3(x)\, T^3 . \tag{6a}$$

Fountain and West (1970) confirmed, using particulate basalt in vacuum, that the thermal conductivity is indeed a function of both temperature and density (therefore, depth) and provided extensive data to determine $k_0(x)$ and $k_3(x)$. By use of these data, these functions are represented very well for calculational purposes by third-degree polynomials, determined by the least-squares technique, of the form

$$k_0(x) = c_0 + c_1\varrho(x) + c_2\varrho^2(x) + c_3\varrho^3(x)$$

and

$$k_3(x) = b_0 + b_1\varrho(x) + b_2\varrho^2(x) + b_3\varrho^3(x), \tag{6b}$$

where

$$\begin{aligned} c_0 &= 0.40627783 \times 10^{-2}\ \mathrm{W\ m^{-1}\ K^{-1}}, \\ c_1 &= -0.10295491 \times 10^{-4}\ \mathrm{W\ m^2\ kg^{-1}\ K^{-1}}, \\ c_2 &= 0.91660767 \times 10^{-8}\ \mathrm{W\ m^5\ kg^{-2}\ K^{-1}}, \\ c_3 &= -0.22511580 \times 10^{-11}\ \mathrm{W\ m^8\ kg^{-3}\ K^{-1}}; \end{aligned} \tag{6c}$$

and

$$\begin{aligned} b_0 &= 0.30821872 \times 10^{-10}\ \mathrm{W\ m^{-1}\ K^{-4}}, \\ b_1 &= -0.18565704 \times 10^{-13}\ \mathrm{W\ m^2\ kg^{-1}\ K^{-4}}, \\ b_2 &= -0.12893852 \times 10^{-16}\ \mathrm{W\ m^5\ kg^{-2}\ K^{-4}}, \\ b_3 &= 0.17879447 \times 10^{-19}\ \mathrm{W\ m^8\ kg^{-3}\ K^{-4}}. \end{aligned} \tag{6d}$$

Equation (6) is adopted for the theoretical model, and comparisons with other data will be made below. Other forms may be used for $k(x, T)$, but they have no better computational accuracy of representation over the full domain of density and temperature for basalt (Fountain *et al.*, 1973).

The specific heat used in Equation (1) is a third-degree polynomial determined by the least-squares technique based upon Apollo 11 data reported by Robie *et al.* (1970) as

$$c(T) = d_0 + d_1 T + d_2 T^2 + d_3 T^3, \tag{7a}$$

where

$$\begin{aligned} d_0 &= -0.05277\ \mathrm{W\ h\ kg^{-1}\ K^{-1}}, \\ d_1 &= 0.15899 \times 10^{-2}\ \mathrm{W\ h\ kg^{-1}\ K^{-2}}, \\ d_2 &= -0.03366 \times 10^{-4}\ \mathrm{W\ h\ kg^{-1}\ K^{-3}}, \\ d_3 &= 0.03142 \times 10^{-7}\ \mathrm{W\ h\ kg^{-1}\ K^{-4}}. \end{aligned} \tag{7b}$$

Table I compares the Apollo 11 values to those calculated using Equation (7), and a comparison with other Apollo data will be mentioned below.

The usual approach for calculating millimeter brightness temperatures whereby the

TABLE I

Specific heat of lunar fines

Temp (K)	Apollo 11, sample 10084 (W s kg^{-1} K^{-1})	Least-squares fit (W s kg^{-1} K^{-1})
100	278.2	272.6
120	335.6	342.0
140	399.6	405.0
160	463.6	462.0
180	516.7	513.8
200	564.0	560.7
220	605.0	603.4
240	641.8	642.4
260	676.6	678.1
280	709.6	711.3
300	741.0	742.4
320	771.9	771.9
340	801.7	800.4

absorption coefficient is regarded as constant and removed from under the integral signs and the physical temperature profile is derived as a Fourier series solution to the homogeneous, linear partial differential equation of heat conduction, does not satisfy the requirements of a variable properties model. The appropriate integral equation for the microwave brightness for the variable model (Ulich *et al.*, 1974) is

$$T_B(\lambda, t) = [1 - R(\theta_0)] \int_0^\infty T(x, t)\, \kappa(\lambda, x) \sec[\theta(x, \theta_0)] \times$$

$$\times \exp\left[-\int_0^x \kappa(\lambda, \xi) \sec\theta(\xi, \theta_0)\, d\xi\right] dx, \tag{8}$$

where $[1-R(\theta_0)]$ is evaluated at $x=0$, $R(\theta_0)$ being the power reflection coefficient for perpendicular incidence at the surface of the thermal emission. The absorption coefficient is

$$\kappa(\lambda, x) = 2\pi\lambda^{-1}\sqrt{\varepsilon(x)}\tan\delta(x), \tag{9}$$

where λ is wavelength, $\varepsilon(x)$ is the dielectric constant, and $\tan\delta(x)$ is the loss tangent. For the variable properties model, $\varepsilon(x)$ and $\tan\delta(x)$ are given by an equation of the form

$$\left.\begin{matrix}\varepsilon(x) \\ \tan\delta(x)\end{matrix}\right\} = \text{constant} + \text{constant}\cdot\varrho(x). \tag{10}$$

The values of the constants in Equation (10) will be discussed in connection with comparisons of the model and observational data below (also, see Ulich *et al.*, 1974).

The reflection coefficient at the lunar surface is determined by the Fresnel equations evaluated at $x=0$, of the form

$$R(\theta_0) = R_{11}(x, \theta_0)\cos^2\gamma + R_{\perp}(x, \theta_0)\sin^2\gamma,$$

where

$$\begin{aligned} R_{11}(x, \theta_0) &= \left[\frac{\varepsilon(x)\cos\theta_0 - \sqrt{\varepsilon(x) - \sin^2\theta_0}}{\varepsilon(x)\cos\theta_0 + \sqrt{\varepsilon(x) - \sin^2\theta_0}}\right]^2, \\ R_{\perp}(x, \theta_0) &= \left[\frac{\cos\theta_0 - \sqrt{\varepsilon(x) - \sin^2\theta_0}}{\cos\theta_0 - \sqrt{\varepsilon(x) - \sin^2\theta_0}}\right]^2; \end{aligned} \tag{11}$$

γ being the polarization angle of the emitted radiation, and $\theta(x, \theta_0)$ is determined by

$$\theta(x, \theta_0) = \arcsin\left[\frac{\sin\theta_0}{\sqrt{\varepsilon(x)}}\right].$$

$T(x, t)$ in the integrand of Equation (8) is obtained from the physical temperature model defined by Equations (1) through (7), generated by the model for a particular time (date) and lunar location corresponding to the millimeter observational data under consideration.

Thus, the radio brightness temperature model is consistent with and dependent upon the variable properties model for the physical temperature.

3. Numerical and Computational Methods

The general approach used here for numerically solving the boundary value–initial condition problem for the physical temperatures is to replace the space derivatives by finite differences in the *pde* and boundary conditions, obtaining a system of ordinary differential-difference equations which are then solved by a method of the one-step type. Henrici (1962) refers briefly to this approach and states (there is no clear proof) that when an equation of higher order (*pde*) is reduced in such a manner to a system of equations of lower order (ord. *de*'s), the truncation error is not increased and the round-off error is usually decreased. The usual explicit finite difference approach in both space and time would, if used, replace the *pde* and boundary conditions with a system of nonlinear transcendental equations whose solution would be extremely difficult (there are no known methods for solution which are practical), whereas the approach used here turns the problem into a tractable one. Fox (1962) also mentions the present approach as being one which might be usefully applied to nonlinear problems of the parabolic type.

When Equation (6a) is substituted into Equation (1), the r.h.s. of the *pde* becomes

$$\begin{aligned} &[k_0(x) + k_3(x)\,T^3]\frac{\partial^2 T}{\partial x^2} + 3k_3(x)\,T^2\left(\frac{\partial T}{\partial x}\right)^2 + \\ &\qquad + \left[\frac{\partial k_0(x)}{\partial x} + T^3\frac{\partial k_3(x)}{\partial x}\right]\frac{\partial T}{\partial x}. \end{aligned} \tag{12}$$

Replacing the partial derivatives by

$$\left.\frac{\partial T}{\partial x}\right|_i \approx \frac{1}{\Delta x_i}\left[T(x_{i+1}, t) - T(x_i, t)\right],$$

$$\left.\frac{\partial^2 T}{\partial x^2}\right|_i \approx \frac{1}{\Delta x_i^2}\left[T(x_{i+1}, t) - 2T(x_i, t) + T(x_{i-1}, t)\right],$$

$$\left.\frac{\partial k_0}{\partial x}\right|_i \approx \frac{1}{\Delta x_i}\left[k_0(x_{i+1}) - k_0(x_i)\right],$$

$$\left.\frac{\partial k_3}{\partial x}\right|_i \approx \frac{1}{\Delta x_i}\left[k_3(x_{i+1}) - k_0(x_i)\right],$$

in which i ($i = 1, 2, 3, \ldots, N-1$) designates the space increment at which the temperature is calculated. The *pde* for the interior of the semi-infinite solid becomes the set of ord. *de*'s of the form

$$\begin{aligned}\frac{\mathrm{d}T(x_i, t)}{\mathrm{d}t} = (1/\Delta x_i^2)&\left[\frac{1 + \left(\frac{\varrho_\infty}{\varrho_0} - 1\right)e^{-x_i/x^*}}{\varrho_\infty c\left[T(x_i, t)\right]}\right]\{k_0(x_{i+1})\left[T(x_{i+1}, t)\right.\\ &- T(x_i, t)] - k_0(x_i)\left[T(x_i, t) - T(x_{i-1}, t)\right]\\ &+ k_3(x_{i+1})\left[T(x_{i+1}, t) - T(x_i, t)\right]T^3(x_i, t)\\ &- k_3(x_i)\left[6T(x_{i+1}, t) - 2T(x_i, t) - T(x_{i-1}, t)\right]T^3(x_i, t)\\ &+ 3k_3(x_i)\,T^2(x_i, t)\,T^2(x_{i+1}, t)\}, \qquad (i = 1, \ldots, N-1).\end{aligned} \tag{13a}$$

In order to incorporate the boundary conditions, a procedure indicated by Ames (1965) is used. The assumption is made that the above *de* for the interior also holds at $i = 0$, and a fictitious layer at $i = -1$ is temporarily introduced. That is, $T(x_{-1}, t)$ is introduced in the de for $T(x_0, t)$ and in the difference equation which replaces the surface boundary condition, Equation (2a). The latter is solved for $T(x_{-1}, t)$ and the result substituted into the former, eliminating the temporary $T(x_{-1}, t)$ and giving the following ordinary differential equation for the surface condition

$$\begin{aligned}\frac{\mathrm{d}T(x_0, t)}{\mathrm{d}t} = &\left(\frac{1 + \left(\frac{\varrho_\infty}{\varrho_0} - 1\right)e^{-x_0/x_0^*}}{\varrho_\infty c\left[T(x_0, t)\right]}\right)\left(\frac{1}{\Delta x_0^2}\right)\left\{k_0(x_1)\left[T(x_1, t)\right.\right.\\ &- T(x_0, t)] - k_0(x_0)\left[T(x_0, t) - T(x_1, t)\right.\\ &\left.\left.- \frac{2\Delta x_0\left[F(t) - \varepsilon\sigma T^4(x_0, t)\right]}{\left[k_0(x_0) + k_3(x_0)\,T^3(x_0, t)\right]}\right]\\ &+ k_3(x_1)\left[T(x_1, t) - T(x_0, t)\right]T^3(x_0, t)\end{aligned} \tag{13b}$$

$$- k_3(x_0)\, T^3(x_0, t)\Bigg[6T(x_1, t) - 2T(x_0, t) - T(x_1, t) - \frac{2\Delta x_0 [F(t) - \varepsilon\sigma T^4(x_0, t)]}{[k_0(x_0) + k_3(x_0)\, T^3(x_0, t)]}\Bigg] + 3k_3(x_0)\, T^2(x_0, t)\, T^2(x_1, t)\Bigg\}. \tag{13b}$$

Similarly, the ordinary differential equation for the interior points is assumed to hold at $x = x_N$, and the assumption is made that $T(x_N, t) = V$ in the resulting de for $T(x_N, t)$, provided only that N is large enough. Also, for N large, $k_0(x_{N+1}) = k_0(x_N)$ and $k_1(x_{N+1}) = k_1(x_N)$. The resulting differential equation for the interior boundary is

$$\frac{dT(x_N, t)}{dt} = \left(\frac{1 + \left(\frac{\varrho_\infty}{\varrho_0} - 1\right) e^{-x_N/x_0^*}}{\varrho_\infty c [T(x_N, t)]}\right)\left(\frac{1}{\Delta x_N^2}\right)\{k_0(x_N)[V - 2T(x_N, t) + T(x_{N-1}, t)] - k_3(x_N)\, T^3(x_N, t)[5V - T(x_N, t) - T(x_{N-1}, t)] + 3k_3(x_N)\, T^2(x_N, t)\, V^2\}. \tag{13c}$$

The set of Equations (13a, b, c) is the system of $N+1$ first order, ordinary differential-difference equations to solve together with the initial conditions given by Equation (4). This set of equations was solved by using a generalized Euler-Rhomberg method obtained by generalizing the Euler-Rhomberg method given by McCalla (1967) for the initial-value problem for one equation. This gives basically a one-step method for solving the time-dependent equations, with iteration between steps, which is self-starting, efficient, allows a predetermined accuracy to be obtained, and permits a variable step size.

A variable space increment is used. The variation is such that the increment increases with increasing depth and allows the increment to be smallest near the surface where the greatest variation in temperature occurs. The following form was found to be computationally suitable:

$$x_i = \sum_{k=0}^{i-1} \Delta x_k, \qquad \Delta x_k = H\left(\frac{x_i}{x_{\max}}\right)^{1/\beta} + \Delta x_0, \tag{14}$$

where $H = \Delta x_{k_{\max}} - \Delta x_0$, β is an integer, and Δx_0 is specified for the particular case of computation. The x_i and Δx_k are determined by iteration between these equations and need be computed only once for each case. A typical graph of the change of the increment with depth is shown in Figure 1.

A variable time step-size is chosen at each step to be as large as possible and still be numerically stable. The stability criteria is based upon a combination of the usual criteria for the linear parabolic problem (Ames, p. 357), the criteria for the nonlinear

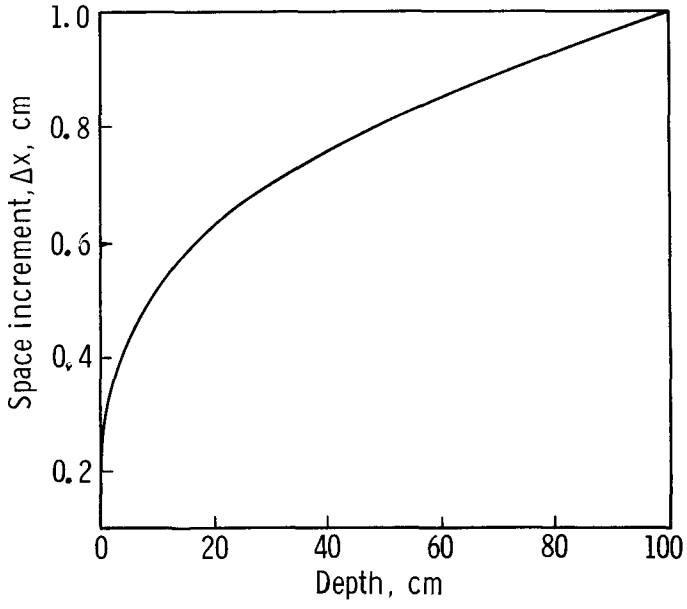

Fig. 1. Example of the change of the space increment with depth.

surface boundary condition (Tatom *et al.*, 1969), and a modification to take account of the variable material properties in this model. The resulting variable time increment for the nth computational step is given by the following:

$$(h_0)_n = \text{Min.}\,\{h_0^*, \text{Min.}\,[(h_0^{**})_i]\}\,, \tag{15}$$

where

$$h_0^* = p\,\frac{\varrho(x_0)\,c[T(x_0, t_n)]\,(\Delta x_0)^2}{k_0(x_0) + k_3(x_0)\,T^3(x_0, t_n) + \Delta x_0 \varepsilon\sigma T^3(x_0, t_n)}\,,$$

$$(h_0^{**})_i = p\,\frac{\varrho(x_i)\,c[T(x_i, t_n)]\,(\Delta x_i)^2}{k_0(x_i) + k_3(x_i)\,T^3(x_i, t_n)}\,,$$

$$(i = 1, \ldots, N) \quad \text{and} \quad p < 0.5\,.$$

In order to calculate the millimeter brightness temperature, Equation (8) is solved by numerical quadrature (Ulich *et al.*, 1974). The physical temperature function, $T(x, t)$, obtained using the model and methods presented here is recorded on magnetic tape and used as input data for the quadrature, so that the calculations are consistent in representing a particular physical case.

For convenience in incorporating an eclipse into the computation, the eclipse function, $E(t/P)$, is represented by cubic splines. An example for the eclipse of December 19, 1964, is shown in Figure 2, where the spline approximations for the two different boundary conditions are also compared with the theoretical curve. One boundary condition is that the first derivative of the function is assumed equal to zero, and the

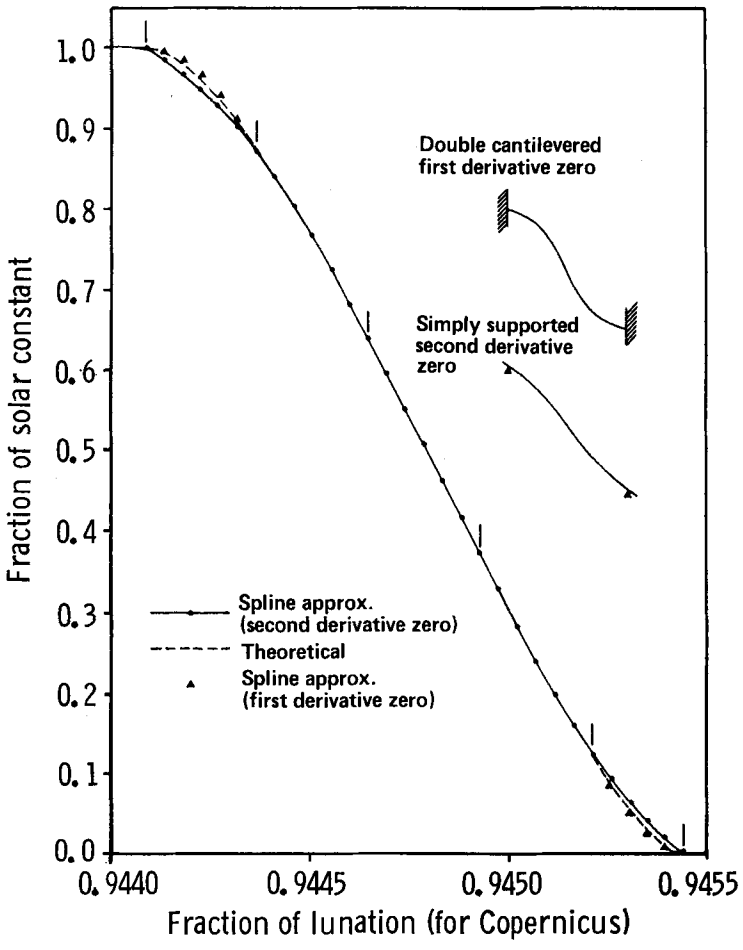

Fig. 2. Cubic spline approximation to the December 19, 1964, eclipse function.

other is that the second derivative is assumed equal to zero. As expected from the physical situation, taking the first derivative to be zero provides the best representation. The theoretical curve is calculated separately and the data used to obtain the spline approximation.

4. Property Data

As previously stated, the data of Fountain and West are incorporated in the thermal conductivity function, Equation (6), and are used for the computations presented here. No other data are defined well enough to obtain an adequate functional relationship using both density (depth) and temperature. The functions $k_0(x)$ and $k_3(x)$ used in the computational case which is central to comparison with the infrared and microwave observational data are shown in Figures 3 and 4. For the same computational

case, Figure 5 shows the thermal conductivity $k(x)$ for three particular temperature-depth profiles corresponding to three particular times in the lunation: namely, at local noon, sunset, and midnight. This set of curves, together with their conditions, gives some idea of the complex interaction of the conductivity function in the theoretical model. The thermal conductivity ranges from 0.6×10^{-5} W cm^{-1} K^{-1} to

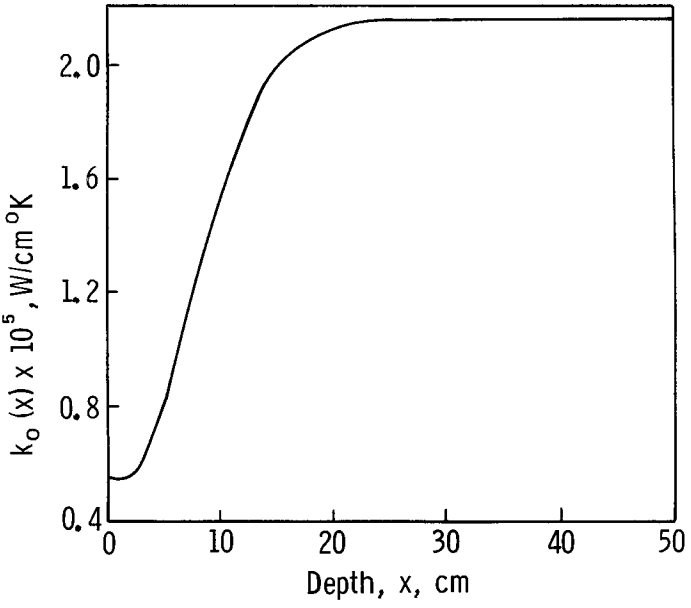

Fig. 3. The depth-dependent coefficient of thermal conductivity, $k_0(x)$.

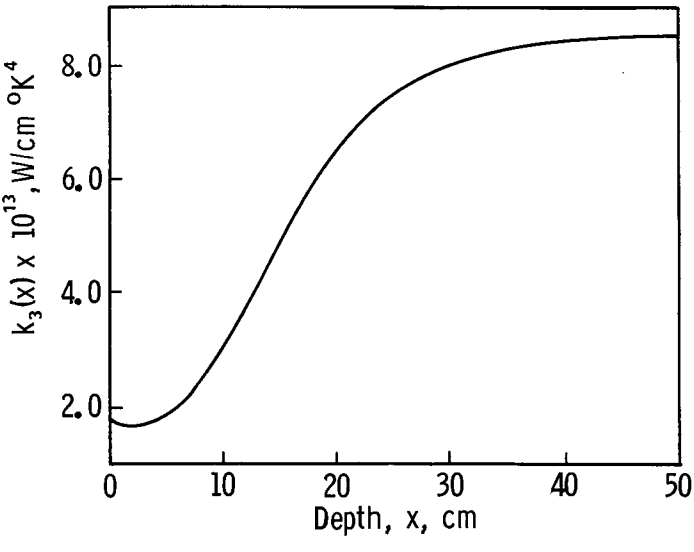

Fig. 4. The depth-dependent coefficient of thermal conductivity, $k_3(x)$.

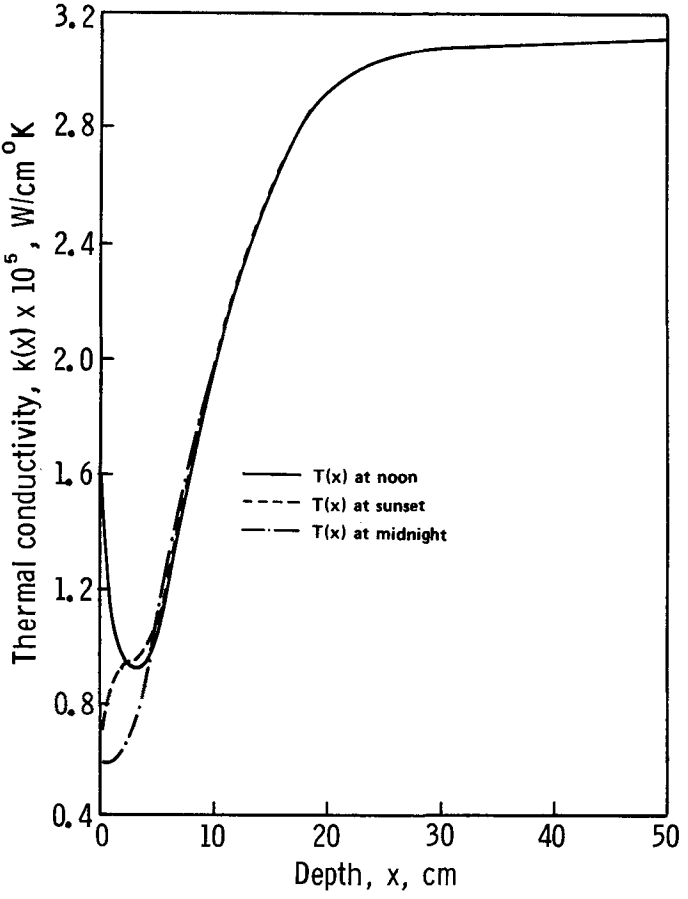

Fig. 5. Thermal conductivity as a function of depth for particular temperature profiles for particular lunation times.

about 3×10^{-5} W cm^{-1} K^{-1}. These conductivity curves correspond to the density-depth profile given by the solid curve in the interior of the shaded area in Figure 14.

The measured conductivity values for samples of lunar fines returned by Apollo range from 0.8×10^{-5} W cm^{-1} K^{-1} to 3×10^{-5} W cm^{-1} K^{-1} over the temperature range of 100 to 400 K and over a density range of 1300 to 1970 kg m^{-3} (Cremers, 1974). The functional form for the conductivity for these samples is $A + BT^3$, and, while there is a functional dependence of some sort of A and B on density, its form is not clear. From data reported (Langseth *et al.*, 1973) on the Apollo 17 Heat Flow Experiment, the upper 2 cm of the lunar surface material has a conductivity estimated to be 1.5×10^{-5} W cm^{-1} K^{-1} at the Taurus-Littrow site, corresponding to a 'loosely packed layer'. At depth, the thermal conductivity is on the order of a factor of 10 higher, corresponding to greater density (1800 to 2000 kg m^{-3}).

Most of the heat flow through the lunar outermost layer is controlled by the thermal

TABLE II

Average conductivity of a mixture of rocks and fines compared with the conductivity of fines

Volume-fraction of rocks α	Ratio of conductivities k_{av}/k
0.00	1.00
0.01	1.03
0.02	1.06
0.03	1.09
0.04	1.12
0.05	1.16

properties of the fine material, because it is the most insulating. It is instructive to estimate the contribution of smaller rocks mixed with the fines on the effective thermal conductivity. Using an approximation based upon the volume fraction of rocks (Carslaw and Jaeger, 1959) assumed to be spheres embedded in a matrix of granular material, Table II shows the ratio of the average conductivity of the mixture to the

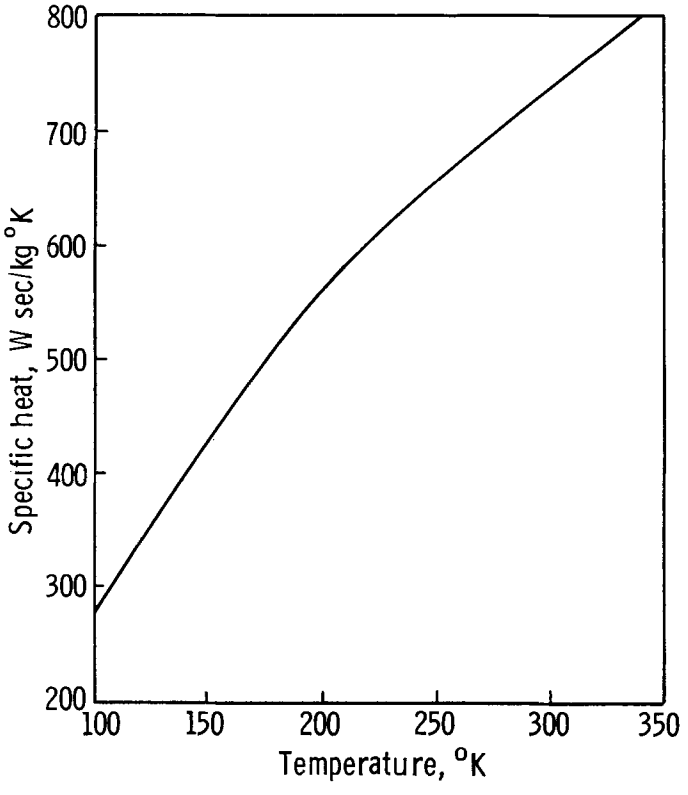

Fig. 6. Specific heat as a function of temperature (calculated from polynomial representation).

conductivity of the granular matrix as a function of volume-fraction of rocks.

As previously stated, Equation (7) is used for the specific heat function based upon the data in Table I. The graph of this function is shown in Figure 6. Although this function is based upon Apollo 11 fines (Robie, 1970), there is essentially no difference between the specific heat values for the fines and the measured values for samples of solid materials from the various Apollo sites, as is pointed out in detail by Cremers (1974), so that this function is entirely suitable for the calculations presented here.

Taking the thermal conductivity and specific heat function as stated, the density profile becomes the primary function to distinguish computation cases for comparison with the observational infrared and microwave data.

5. Comparison of Calculated and Observation Temperatures

Over twenty-five different density profiles were used as the basis for computational cases for lunations. The characteristics of seventeen of these are given in Table III; the average density given is obtained by integration of the density function in each case.

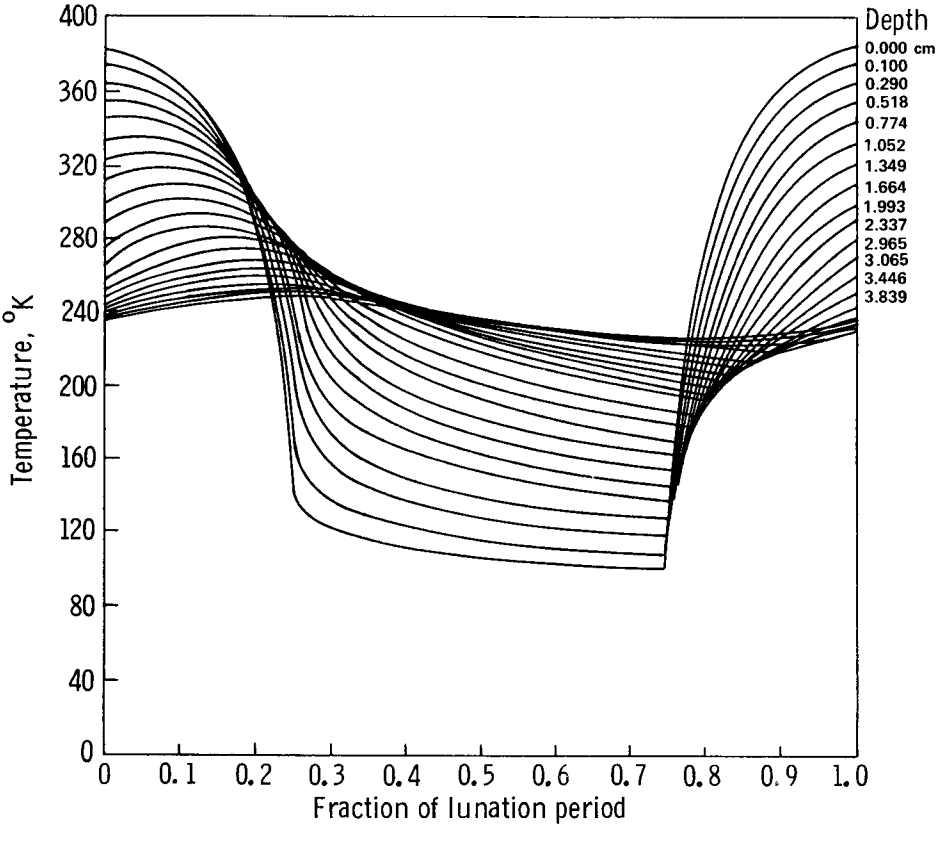

Fig. 7. Calculated temperatures for a typical case.

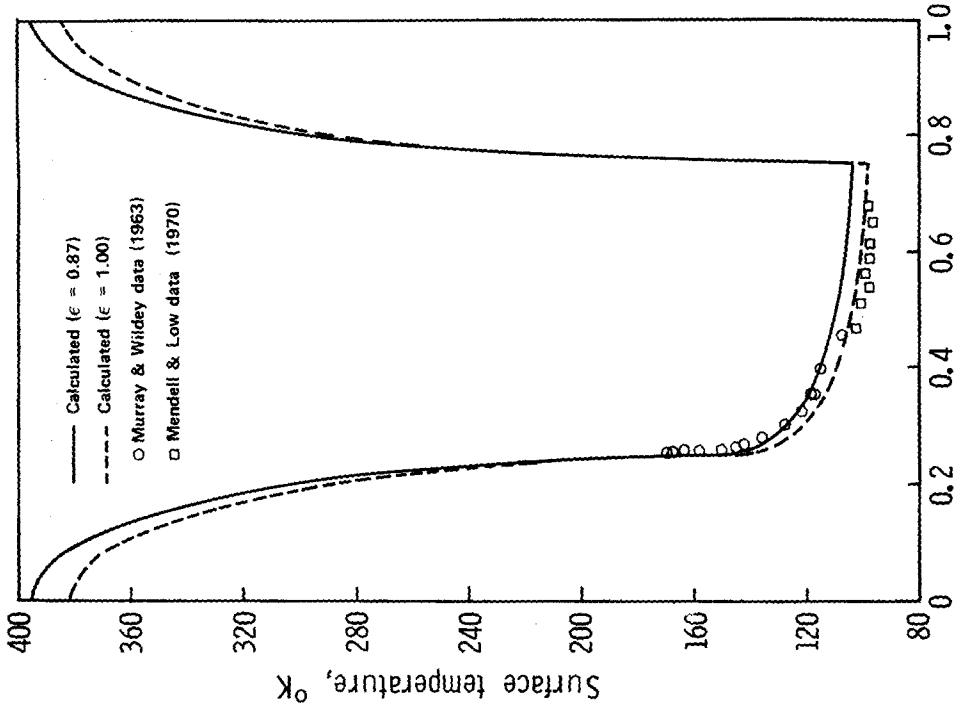

Fig. 9. Comparison of observed infrared and calculated temperatures (Case A, Table III).

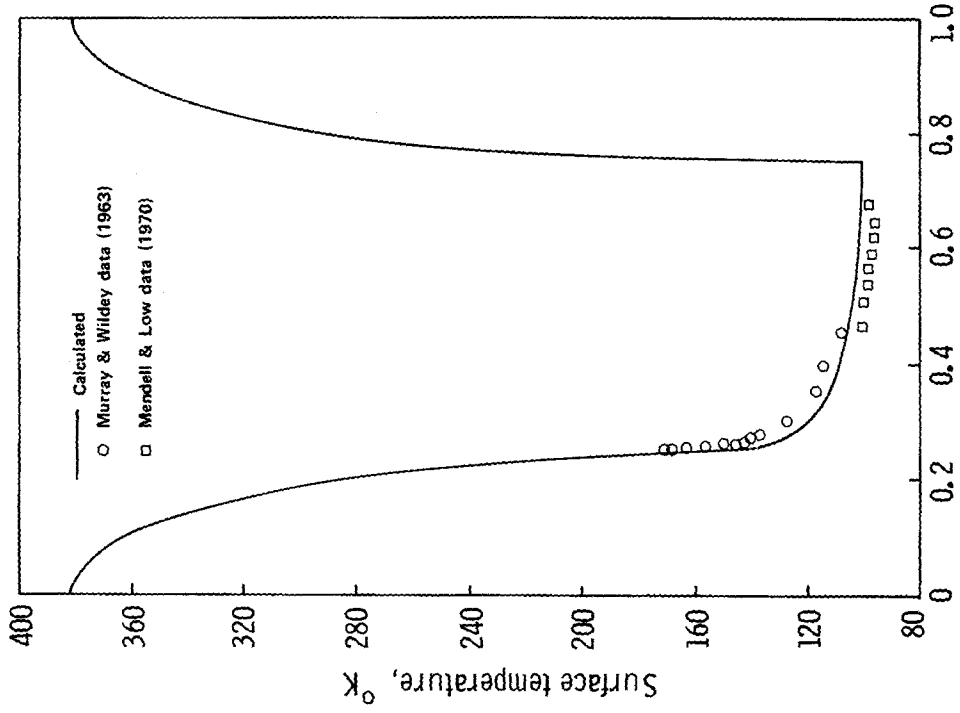

Fig. 8. Comparison of observed infrared and calculated temperatures (Case B, Table III).

TABLE III

Average density for various parameters of the density model

ϱ_0 (kg m^{-3})	ϱ_∞ (kg m^{-3}	x_{int} (m)	ϱ_{int} (kg m^{-3})	x^* (m)	ϱ_{av} (kg m^{-3})
700	1300	0.01	1000	0.0095	1262
700	1700	0.05	1000	0.0702	1218
700	1700	0.01	1000	0.0140	1594
700	1700	0.02	1000	0.0280	1489
700	1700	0.03	1000	0.0421	1387
700	1700	0.04	1000	0.0561	1296
700	1700	0.10	1045	0.1405	994
800	1700	0.05	1000	0.1053	1165
600	2000	0.04	1000	0.0472	1447
B600	2000	0.09	1700	0.0349	1586
600	2000	0.25	1100	0.2386	957
600	2000	0.25	900	0.3867	380
700	2000	0.02	1000	0.0323	1662
700	2000	0.03	1000	0.0485	1506
A700	2000	0.04	1000	0.0646	1374
800	2000	0.04	1000	0.0989	1274
900	2000	0.04	1000	0.1991	1147

Calculated temperatures as a function of depth and time for a lunation for a typical case are shown in Figure 7, where it is seen that the large gradients near the surface are satisfactorily taken into account by the numerical and computational methods used. Here, and in the cases presented below, the solar radiation absorptance is 0.93 and the value for V is 251 K. This value for the lower boundary temperature is from the measurements by the Apollo 15 Heat Flow Experiment (Langseth *et al.*, 1972).

A comparison of the calculated surface temperature for the case B in Table III and the infrared data of Murray and Wildey (1963) and that of Mendell and Low (1970) is made in Figure 8. The density profile for this case is the upper bounding curve of the cross-hatched region in Figure 14. In Figure 9, the same data are compared with the calculated temperatures for case A in Table III for two different values of the emittance of the lunar surface. The density profile for this case is represented by the solid curve in the interior of the shaded region in Figure 14. For this same case A, the calculated temperatures are compared with the infrared eclipse measurements of Saari and Shorthill for the eclipse of December 19, 1964, in Figure 10 (Shorthill and Saari, 1965, 1967). The comparison with the same eclipse data and case B is made in Figure 11.

The calculated temperatures as a function of depth and time from the model presented here were used (via magnetic tape) in the integrand of Equation (8), for the same density profile of case A (Table III), to calculate microwave brightness temperatures at 3.09 mm wavelength. The calculated temperatures are compared with the data of Ulich *et al.* for the Apollo 11 and 12 sites in Figures 12 and 13, respectively. Comparisons with data for other lunar locations were presented by Ulich *et al.* (1974)

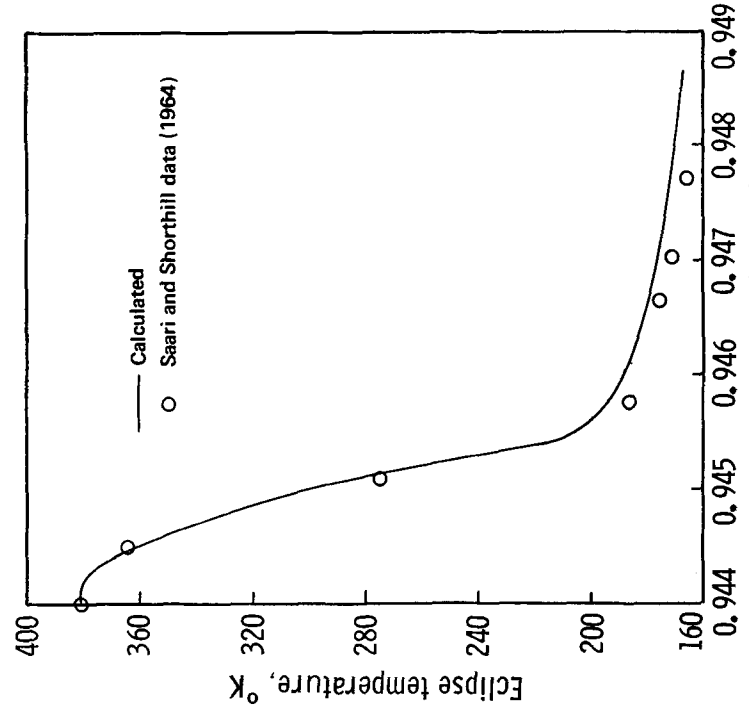

Fig. 11. Comparison of calculated and infrared eclipse temperatures for the December 19, 1964, eclipse (Case B, Table III).

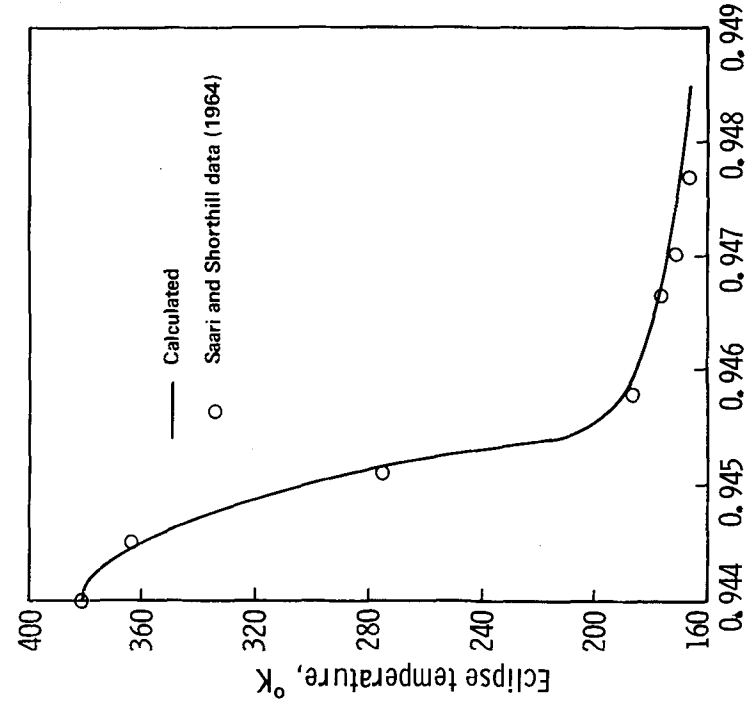

Fig. 10. Comparison of calculated and infrared eclipse temperatures for the December 19, 1964, eclipse (Case A, Table III).

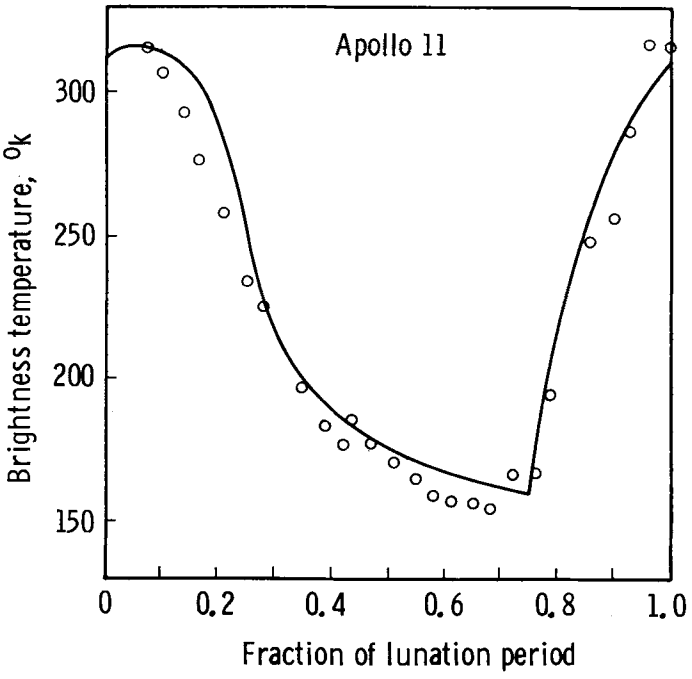

Fig. 12. Comparison of calculated and observed brightness temperatures at 3.09 mm wavelength for the Apollo 11 site.

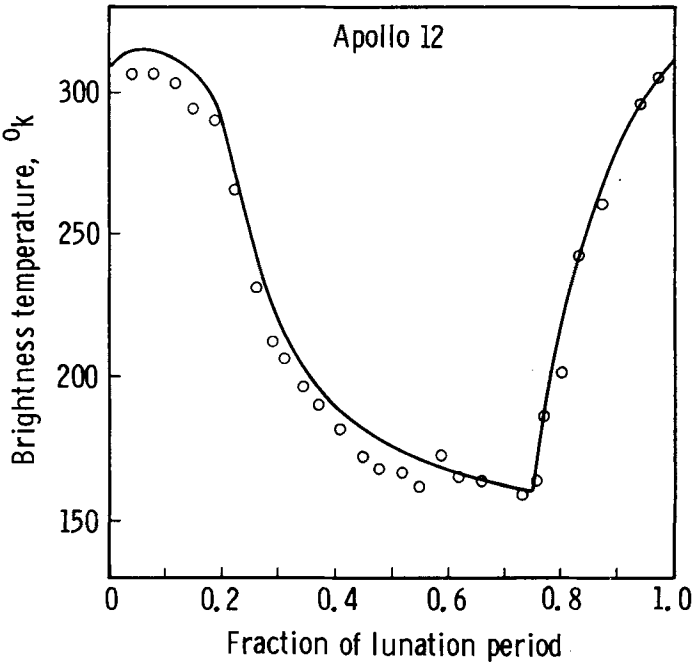

Fig. 13. Comparison of calculated and observed brightness temperatures at 3.09 mm wavelength for the Apollo 12 site.

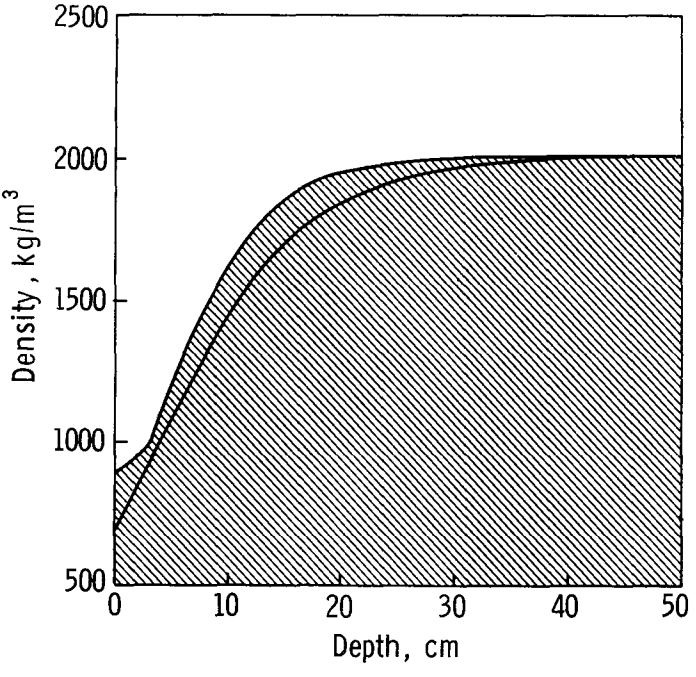

Fig. 14. Region of density profiles consistent with calculated and observed lunar temperatures.

and should be considered in conjunction with these results since those comparisons depend upon the physical models and temperatures presented here.

The upper bounding curve for the density profile in Figure 14 represents the limiting profile which will allow favorable comparison with the infrared and microwave observational data. The first part of the curve, corresponding to about the first three or four centimeters of depth, influences the infrared comparisons most strongly, while the remainder of the curve most strongly influences the microwave comparisons.

6. Conclusions

The variable properties model presented here is consistent with the known properties of the lunar outermost layer, and the calculated temperatures compare well with the most recent Earth-based observational data in the infrared and at millimeter wavelengths. The density profile in the outermost layer very probably varies from 700 to 900 kg m^{-3} at the surface, rising rapidly to about 2000 kg m^{-3}. For the purposes of comparison with Earth-based data, further sophistication of the thermophysical model is probably not justified.

References

Ames, W. F.: 1965, *Nonlinear Partial Differential Equations in Engineering*, Academic Press, New York, p. 357.

Buettner, K. J. K.: 1963, *Planetary Space Sci.* **11**, 135–148.
Calvert, T. A.: 1969, NASA TM X-1734, p. 38.
Carslaw, H. S. and Jaeger, J. C.: 1959, *Conduction of Heat in Solids*, Second Edition, Oxford Univ. Press, London, p. 428.
Cremers, Clifford J.: 1974, in James P. Hartnett and Thomas F. Irvine, Jr. (eds.), *Advances in Heat Transfer*, Academic Press, Inc., New York, pp. 39–83.
Epstein, P.: 1929, *Phys. Rev. Abstracts* **33**, 269.
Fountain, J. A. and West, E. A.: 1970, *J. Geophys. Res.* **75**, 4062–4069.
Fountain, J. A., Scott, R. W., and West, E. A.: 1973, NASA TM X-64759.
Fox, L.: 1962, *Numerical Solution of Ordinary and Partial Differential Equations*, Pergamon Press, New York, pp. 240–242 and 252.
Halajian, J. D., Reichman, J., and Karafiath, L. L.: 1967, Research Report RE-280, Grumman Aircraft, Bethpage, N.Y.
Henrici, P.: 1962, *Discrete Variable Methods in Ordinary Differential Equations*, John Wiley and Sons, Inc., New York, pp. 109–110.
Jones, B. P.: 1968, *J. Geophys. Res.* **73**, No. 24, 7631–7635.
Jones, B. P.: 1969, in J. T. Bevans (ed.), *Progress in Astronautics and Aeronautics: Thermal Design Principles of Spacecraft and Entry Bodies*, Academic Press, New York, pp. 469–487.
Langseth, Marcus G., Jr., Clark, S. P., Chute, J. Jr., and Keihm, S.: 1972, *3rd Lunar Science Conference: Abstracts* (Jan. 10–13, 1972), pp. 422–424; also, *Apollo 15 Preliminary Science Report*, NASA SP-289, pp. 11-1, 11-23.
Langseth, Marcus G., Jr., Keihm, S. J., and Chute, J. L., Jr.: 1973, *Apollo 17 Preliminary Science Report*, NASA SP-300, p. 9-22.
Linsky, J. L.: 1966, *Icarus: International J. of the Solar System* **5**, No. 6, 606–634.
McCalla, Thomas Richard: 1967, *Introduction to Numerical Methods and FORTRAN Programming*, John Wiley and Sons, Inc., New York, pp. 341–348.
Mendell, W. W. and Low, F. J.: 1970, *J. Geophys. Res.* **75**, No. 17, 3319–3324.
Murray, B. C. and Wildey, R. L.: 1963, Contribution No. 1173, Division of Geological Sciences, Calif. Inst. of Tech., Pasadena, Calif., p. 28.
Murray, B. C. and Wildey, R. L.: 1964, *Astrophys. J.* **139**, 734–750.
Pettit, E. and Nicholson, S. B.: 1930, *Astrophys. J.* **71**, 102.
Robie, R. A., Hemingway, B. S., and Wilson, W. H.: 1970, *Science* **167**, No. 3918, 749–750.
Saari, J. M. and Shorthill, R. W.: 1967, in S. F. Singer (ed.), *Physics of the Moon*, Vol. 13, AAS Science and Technology Series, pp. 57–99.
Shorthill, R. W. and Saari, J. M.: 1965, *Science* **150**, 210–212.
Tatom, F. B., Deshpande, P. B., Hung, F. T., and Vaughan, O. H.: 1969, in Jerry T. Bevans (ed.), *Thermal Design Principles of Spacecraft and Entry Bodies*, Academic Press, New York, p. 348.
Troitskiy, V. S.: 1965, *J. Res. Natl. Bur. Stand.* **16D**, 1585–1612.
Troitskiy, V. S. and Tikhonova, T. V.: 1971, NASA TT F-13, 455, January 1971, p. 61. (Translation of Izvestiya vysshikh uchebuykh zavedeniy, *Radiofizika* **13**, No. 9, 1273–1311, 1970.
Ulich, B. L., Cogdell, J. R., Davis, J. H., and Calvert, T. A.: 1974, *The Moon* **10**, No. 2, 163–174.
Watson, K.: 1964, Ph.D. Dissertation, California Institute of Technology, Pasadena, California.
Weaver, Harold: 1965, in Jules Aarons (ed.), *Solar System Radio Astronomy*, Plenum Press, New York, p. 295.
Wechsler, A. E. and Simon, I.: 1966, Contract Report NAS8-20076, Arthur D. Little, Inc., Cambridge, Mass.
Wesselink, A. J.: 1948, *Bull. Astron. Inst. Neth.* **X**, 390, 351–363.
Wildey, R. L.: 1967, *J. Geophys. Res.* **72**, No. 18, 4765–4767.
Winter, D. F.: 1968, Boeing Scientific Research Laboratories Document, D1-82-0717.
Winter, D. F. and Saari, J. M.: 1969, *Astrophys. J.* **156**, 1135–1151.